

Final Draft
of the original manuscript:

Fitseva, V.; Hanke, S.; dos Santos, J.F.:

**Influence of rotational speed on process characteristics in friction
surfacing of Ti-6Al-4V**

In: Materials and Manufacturing Processes (2016) Taylor & Francis

DOI: 10.1080/10426914.2016.1257799

**The 30th International Conference on
Surface Modification Technologies (SMT30)**

29TH JUNE - 1ST JULY, 2016, MILAN, ITALY

**INFLUENCE OF ROTATIONAL SPEED ON PROCESS
CHARACTERISTICS, MATERIAL FLOW AND MICROSTRUCTURE
EVOLUTION IN FRICTION SURFACING OF TI-6AL-4V**

V. Fitseva*, S. Hanke, J.F. dos Santos

Helmholtz-Zentrum Geesthacht GmbH, Institute of Materials Research, Materials Mechanics, Solid State
Joining Processes, Max-Planck Str.1, 21502 Geesthacht, Germany

Abstract

Friction Surfacing is a process employed to deposit metallic coatings, whereby similar and dissimilar material combinations can be realized. The process can be applied as a local repair technology or the coating material can locally modify the surfaces. One advantage of this process is that the coatings are deposited in solid state without reaching the melting range of materials, thereby avoiding dilution with the substrate. The involved severe plastic deformation under high temperatures alters the microstructure of the coating material, leaving it fully dynamically recrystallized.

The current work focuses on deposition of Ti-6Al-4V coatings. For this material the process parameter rotational speed plays a significant role in the material's response during processing. Two different regimes with a threshold at 2000 min⁻¹ exist, upon which the flow behaviour of Ti-6Al-4V significantly differs, affecting amongst others the coating dimensions. Microstructural analysis reveals that the material is deformed in high temperature β phase, and the high cooling rates (46.4 Ks⁻¹) lead to martensitic transformation. The β grain size differs in the low and high rotational speed regime. This study shows that metallurgical processes play an important role in Friction Surfacing, since they influence all relevant process characteristics, including microstructure, material efficiency and process forces.

Keywords: Friction Surfacing, Ti-6Al-4V, microstructure, cooling rates, thermo-mechanical process, dynamic recrystallization

1. Introduction

The Friction Surfacing (FS) process has been known since the 1950s and numerous material combinations have been effectively processed by this technique (Rafi et al. (2010), Hanke et al. (2013), Hanke et al. (2009), Puli et al. (2012), Rao et al. (2012), Suhuddin et al. (2012) and Fitseva et al. (2015)). Friction Surfacing can be employed for local material modifications or as a repair method for worn or otherwise damaged metallic parts. The process has been industrially implemented for the modification of steel microstructure and properties during the manufacturing of knives with increased wear resistance for the packing and processing industry (2010).

Metallic materials can be deposited by Friction Surfacing without reaching the melting range. Due to the relatively low temperatures reached by FS, in comparison to fusion welding, the residual stresses induced into the coated components are low.

During FS, a cylindrical consumable rod is brought onto the substrate to be coated under a pre-set axial force and rotational speed (Figure 1). Through friction, localized heat generation occurs, followed by the plastification of the consumable rod tip. When a traversal movement of the substrate is superimposed, the plasticised material of the rod tip is sheared off and is deposited behind the rod. Excessive plasticized material climbs up around the rod, and forms a flash.

*Corresponding author. Tel.: +49-415287-2065; fax: +49-415287-2033.
E-mail address: viktoria.fitseva@hzg.de

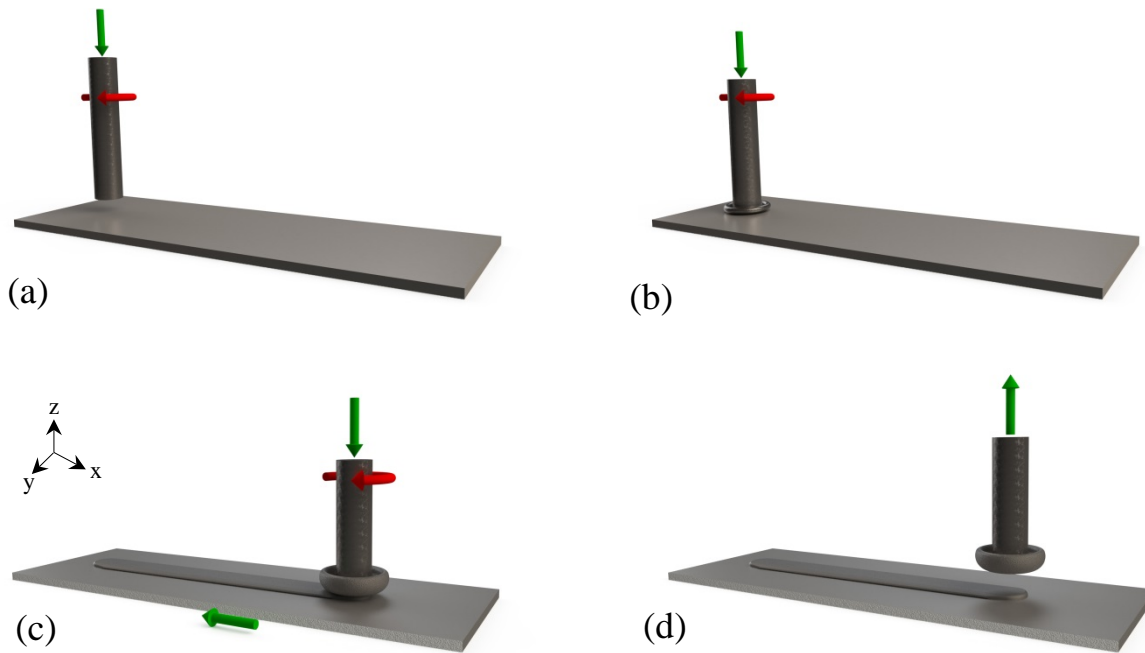


Figure 1: Schematic of FS process described in four steps. (a) Positioning of the consumable rod, (b) plastification phase under axial load and rotational speed, (c) coating is deposited onto the substrate, (d) ramp up of the rod

The possibility of depositing titanium alloy Ti-6Al-4V by Friction Surfacing has recently been reported by Fitseva et al. (2015). Titanium alloys are known to exhibit a complex deformation behavior and tend to flow instabilities. During the development of the FS process for Ti-6Al-4V alloy, several interesting features of temperature evolution, process reaction forces and coating appearance were observed. Since earlier investigations on the behavior of Ti-6Al-4V under comparably high strains, strain rates and temperatures as encountered during Friction Surfacing are very limited, the current work is targeted at analysing the material response to the process parameters, in particular the rotational speed, and the corresponding microstructure development in the coating material.

2. Experimental details

The FS equipment used for the current study has been custom-designed with a high stiffness for high process loads and is capable of delivering 60 kN axial force, 6000 min^{-1} rotational speed and 200 Nm of torque. It can be operated not only in a force control but also in the rod consumption rate controlled mode (RCR, i.e. shortening of the rod per unit of time, also denominated as the burn-off rate). Sensors for monitoring of torque and forces in all three directions are implemented at the FS equipment for monitoring of the measured data. The working space measuring 0.5 m x 1.5 m and a maximum length of the consumable rod of 500 mm enables the coating of larger components. The machine is equipped with a flash cutting device to trim excessive plasticised material off the rod, which otherwise would block rod feeding.

Due to the high chemical affinity of titanium alloys to oxygen at temperatures above 400 °C, argon was used as shielding gas to avoid the formation of a brittle oxide layer and the contamination of the rod and the substrate from the atmosphere.

Ti-6Al-4V alloy was used as a consumable rod in rolled condition and hot-rolled plates were used as substrate. The substrate dimensions are 300 mm x 100 mm x 10 mm and the consumable rod has a diameter of 20 mm at a length of 500 mm. The chemical composition and mechanical properties of the used material (rod and plate) determined by optical spark emission and standard tensile tests (DIN 50125-A 12 x 60) are presented in Table 1 and Table 2, respectively.

Table 1: Chemical composition of the base materials (wt. %)

	Material	Fe	C	N	H	O	Al	V	Ti
Consumable rod	Ti-6Al-4V	0.11	0.03	0.023	0.003	0.15	6.6	3.5	Bal.
Substrate	Ti-6Al-4V	0.11	0.02	0.007	0.004	0.049	6.2	3.9	Bal.

Table 2: Mechanical properties of the base materials

	Material	Tensile strength [MPa]	Elongation [%]
Consumable rod	Ti-6Al-4V	910 ± 8	13.11 ± 1
Plate	Ti-6Al-4V	830 ± 8	12 ± 2

Temperature measurements were obtained with an infrared camera (InfraTec, ImageIR 8300) during the depositions. The infrared camera was placed in front of the FS machine and was focused on the rod tip. The emission factor ϵ was determined for Ti-6Al-4V alloy using a furnace, and was found to vary between 0.75 and 0.89, depending on the temperature, in a range of 800 °C to 1300 °C.

Cross sections of the deposits have been prepared according to standard metallographic practices. After grinding and polishing, the samples with geometry of 10 x 5 x 3 mm were prepared using a Cross Section Polisher (JEOL IB-09010CP) to remove any deformed layer from mechanical preparation. The milling parameters for titanium alloy of a voltage of 6 kV, a gas flow of 5.2 and a milling duration of 6 hours have been found to be suitable.

Scanning Electron Microscopy (SEM) (QuantaTM 650 FEG) was employed to investigate the coatings' microstructure by Electron Backscatter Diffraction (EBSD) (Hikari XP). In order to visualize the prior high temperature β grain boundaries after their transformation to α during cooling of the deposited material, grain boundary reconstruction was carried out based on the method suggested by Gey et al.(2002). The main aim of this method is to distinguish the prior β grain boundaries from other high angle boundaries by a classification of misorientations between α variants inherited from the same parent β -grain, according to Burgers orientation relationship. Following angles with individual planes have been selected for Ti-6Al-4V alloy: $60^\circ\langle 11\bar{2}0\rangle$, $60.83^\circ\langle 1.377; \bar{1}; 2.377; 0.359\rangle$, $63.26^\circ\langle \bar{1}0; 5; 5; \bar{3}\rangle$ and $90^\circ\langle 1; \bar{2}.38; 1.38; 0\rangle$ (Mironov et al. (2008), Gey et al. (2003), Glavicic et al. (2003), Gey et al. (2002)). The contours of the prior β grain boundaries can be reconstructed by eliminating the supernatant boundaries from the EBSD map. Eventually, a black and white map is created showing exclusively the prior β grain boundaries, excluding the martensitic features.

3. Results and discussion

1.1 Coating appearances at different rotational speeds

The initial process development to deposit Ti-6Al-4V alloy coatings using a consumption rate control mode has been published earlier (Fitseva et al. (2015)). The current work is based on the investigation of the influence of rotational speed and deposition speed on the deposited material. The rotational speed was varied in a wide range, between 400 min⁻¹ and 1000 min⁻¹ in steps of 100 min⁻¹, and from 2000 min⁻¹ to 6000 min⁻¹ in steps of 1000 min⁻¹. The consumption rate (1.6 mm/s) was kept constant. The occurring appearances of coatings, generated in the wide range of rotational speeds at a constant deposition speed of 16 mm/s, are demonstrated in Figure 2.

Coatings with smooth surface without visible oxide layer were observed for 300 min⁻¹ to 600 min⁻¹ rotational speed. When increasing the rotational speed in a range of 700 min⁻¹ to 1000 min⁻¹, discontinuous coatings with flash formation and tempering colours at the flash material were formed. The flash formation at the coatings produced is suppressed at higher rotational speed (2000 min⁻¹ – 6000 min⁻¹) and the surface is rough and oxidized, demonstrating a typical FS coating appearance.



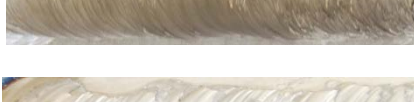


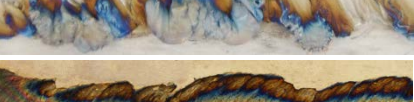
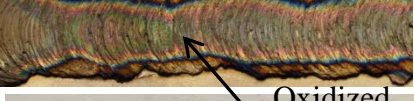
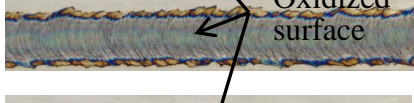
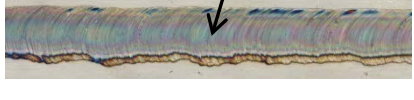
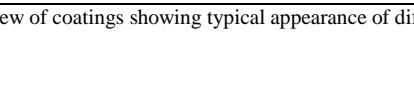
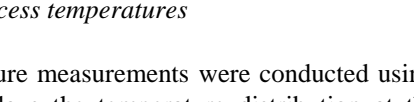
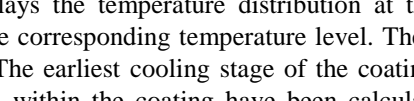
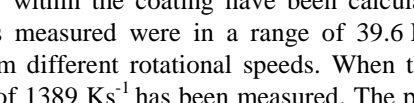
Rot. speed [min ⁻¹]	Coating appearance at 16 mm/s deposition speed, 1.6 mm/s consumption rate
300	
400	
500	
600	
700	
800	
900	
1000	
2000	
3000	
4000	
5000	
6000	

Figure 2: Top view of coatings showing typical appearance of different rotational speed regimes for Ti-6Al-4V

1.2 Process temperatures

Temperature measurements were conducted using an infrared camera. A thermal image captured during the process displays the temperature distribution at the rod tip and in the coating (Figure 3). The color scale represents the corresponding temperature level. The maximum temperature (1377 °C) has been achieved in the shear zone. The earliest cooling stage of the coating behind the rod exhibits a temperature of 1178.2 °C. The cooling rates within the coating have been calculated from the maximum temperature down to 200 °C. The cooling rates measured were in a range of 39.6 Ks⁻¹ to 46.4 Ks⁻¹ depending on the maximum temperature resulting from different rotational speeds. When the highest rotational speed of 6000 min⁻¹ was employed, a heating rate of 1389 Ks⁻¹ has been measured. The process temperature exceeded the β -transus temperature in all experiments. The peak temperature reached a steady-state condition while processing, staying constant throughout the complete deposition process. Furthermore, it was found that regardless of the used parameters, the process temperature during FS of Ti-6Al-4V cannot be suppressed below the β transformation temperature.

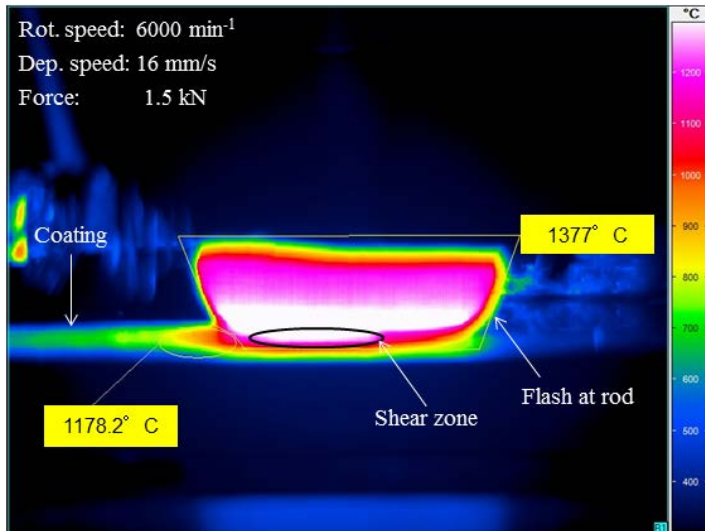


Figure 3: Temperature distribution measured by IR camera during the process indicating maximum temperatures in the process zone and at the coating behind the rod (in the initial cooling stage)

The maximum temperatures measured in the process zone for different rotational speeds are presented in Figure 4. An increase in temperature with rotational speed can be observed, until the temperature reaches its maximum at 2000 min^{-1} . Following this, the temperature has achieved a plateau and remains constant with further increase in rotational speed. This temperature trend at high rotational speeds is contrary to the temperature trend measured by thermocouples (Fitseva et al. (2015)). These differences may be related to the position in which the temperatures were measured. The thermocouples were placed in the interface between the coating and the substrate, while using the infrared camera the temperature within the shear zone was detected. The constant temperature in the shear zone at high rotational speeds (2000 min^{-1} to 6000 min^{-1}) can be explained assuming that no further heat is generated with increasing shear rate, once a certain “viscous” material condition is reached.

Interestingly, the temperature achieved its maximum at that rotational speed, at which the flash formation at the coating is precluded. The flash formation will be discussed in detail in the following section.

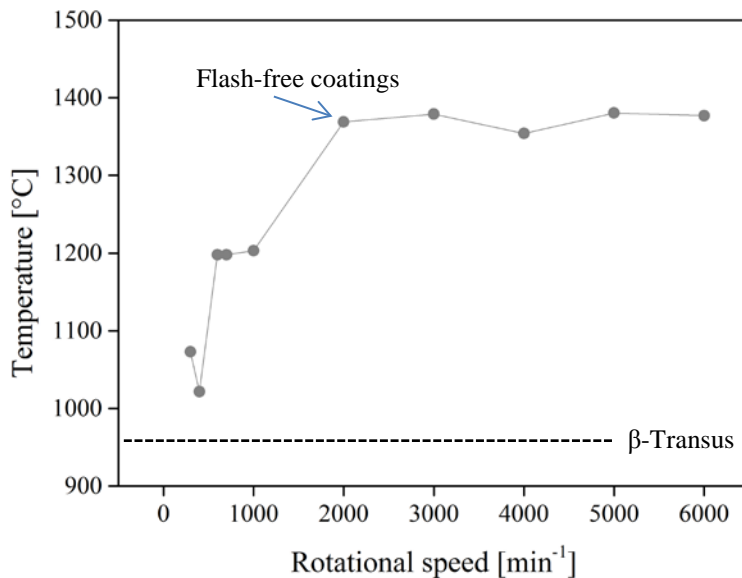


Figure 4: Maximum temperature in the process zone of Ti-6Al-4V alloy coatings as a function of the rotational speed. Temperature has achieved steady-state condition at 2000 min^{-1}

1.3 Process response in two different rotational speed regimes

Generally, while depositing coatings by FS, the flash forms primarily at the consumable rod, ascending around the tip and leaving the coating without flash material (Figure 5). In case of titanium coatings however, as mentioned earlier, under certain rotational speeds (300 min^{-1} - 1000 min^{-1}) the flash is deposited along the retreating side (where the rotational velocity vector is contrary to the deposition direction) of the layer leaving the rod tip without flash (Figure 6).

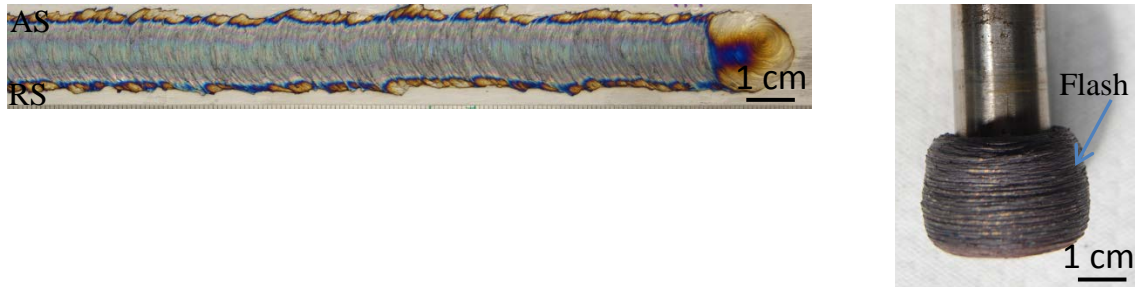


Figure 5: Top view of FS coating generated with 3000 min^{-1} rotational speed, 16 mm/s deposition speed and 1.8 mm/s consumption rate and corresponding consumable rod with flash formation

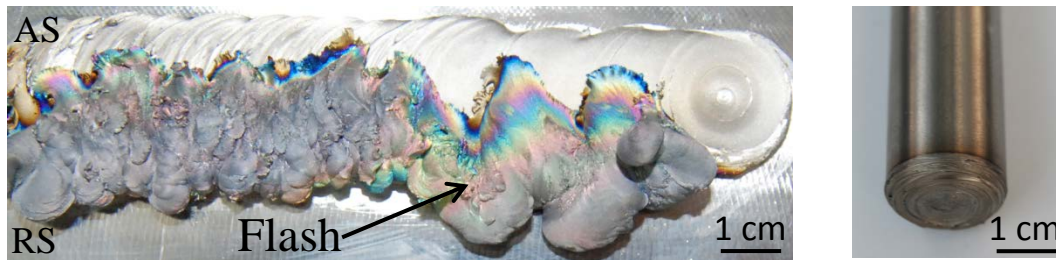


Figure 6: Top view of FS coating generated with 900 min^{-1} rotational speed, 12 mm/s deposition speed and 1.8 mm/s consumption rate displaying flash formation at the RS, and corresponding consumable rod without flash

According to the coating appearances demonstrated in Figure 2 and the temperature evolution for different rotational speeds (Figure 4), a threshold at 2000 min^{-1} rotational speed can be observed. This threshold is consistent with the flash formation at the coating dividing the rotational speed range into two regimes:

- low rotational speed range (300 min^{-1} – 1000 min^{-1}), where the flash may form either at the coating or at the consumable rod (regime I)
- high rotational speed range (2000 min^{-1} – 6000 min^{-1}), where the flash forms exclusively at the consumable rod (regime II).

The material flow of titanium coatings changes in both regimes. As it is well known, the plastic deformation flow stress of metals differs depending on the temperature. At the same time it can be assumed, that flow stresses must affect the axial force acting during processing. It has been demonstrated that temperature alters with rotational speed by FS in regime I. To clarify the influence of deposition speed on temperature evolution, additional experiments were conducted. The deposition speed was varied from 8 mm/s to 16 mm/s at a rotational speed of 400 min^{-1} in regime I and from 4 mm/s to 16 mm/s at a rotational speed of 3000 min^{-1} in regime II. The influence of the deposition speed on the resultant axial force and temperature at a rotational speed of 400 min^{-1} with corresponding images of the Ti-6Al-4V alloy coatings are presented in Figure 7. It can be observed that coating appearances change; the flash was formed at the coating when the deposition speed of 8 mm/s was employed and the highest maximum temperature ($1286 \text{ }^\circ\text{C}$) was achieved. With an increase in deposition speed to 12 mm/s and to 16 mm/s , the flash formation was precluded. This might be related to a corresponding decrease in temperature ($1063 \text{ }^\circ\text{C}$ and $1052 \text{ }^\circ\text{C}$). Moreover, the resultant axial force also varies in dependence of the employed deposition speed. The axial force ascended from 10 kN to 27 kN with increase in the deposition speed, in correlation to the temperature decrease from $1286 \text{ }^\circ\text{C}$ to $1052 \text{ }^\circ\text{C}$. The high resultant axial forces at high deposition speed might be seen as the colder material's higher shear strength. Moreover, these assumed high flow stresses result in flash-free coatings.

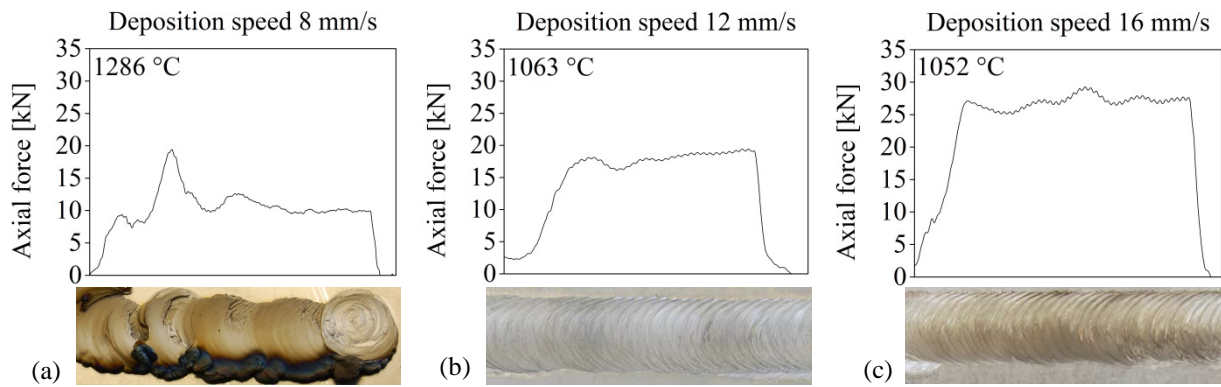


Figure 7: Axial force response to variation of the deposition speed when using 400 min^{-1} rotational speed with corresponding temperature values and Ti-6Al-4V alloy coating images

The effect of the deposition speed on the resultant axial force trend and temperatures at 3000 min^{-1} rotational speed with corresponding coating images is demonstrated in Figure 8. All coatings were deposited without flash formation. At this rotational speed (regime II), a decrease in deposition speed did not influence the material flow behavior in terms of flash formation such as in Figure 7. The force decreases from 6 kN to 2 kN with an increase in deposition speed from 4 mm/s to 16 mm/s, which is contrary to the force evolution with 400 min^{-1} rotational speed. The temperature remained relatively constant measuring $1379 \text{ }^\circ\text{C}$, $1379 \text{ }^\circ\text{C}$ and $1378 \text{ }^\circ\text{C}$ for deposition speeds 4 mm/s, 8 mm/s and 16 mm/s, respectively. It seems that temperature evolution has already achieved its maximum value, as described above, and cannot be altered by the variation in deposition speed. Instead, since the temperature cannot be elevated when employing 4 mm/s deposition speed, the axial force may rise due to a higher strain applied to the consumable rod material. The material at a constant rotational speed undergoes a higher number of rotations before being deposited when using 4 mm/s deposition speed compared to the 16 mm/s. This could raise the fraction of strain hardening in the dynamic recrystallization processes acting during the process, thereby increasing the shear flow stress. Further, it has been reported, that at a low deposition speed the prolonged plastic deformation time causes the formation of a large volume of plasticised material (Rafi et al. (2010)). An increase in the volume of deforming material could also lead to a higher process force of 6 kN for 4 mm/s compared to 2 kN axial force for 16 mm/s.

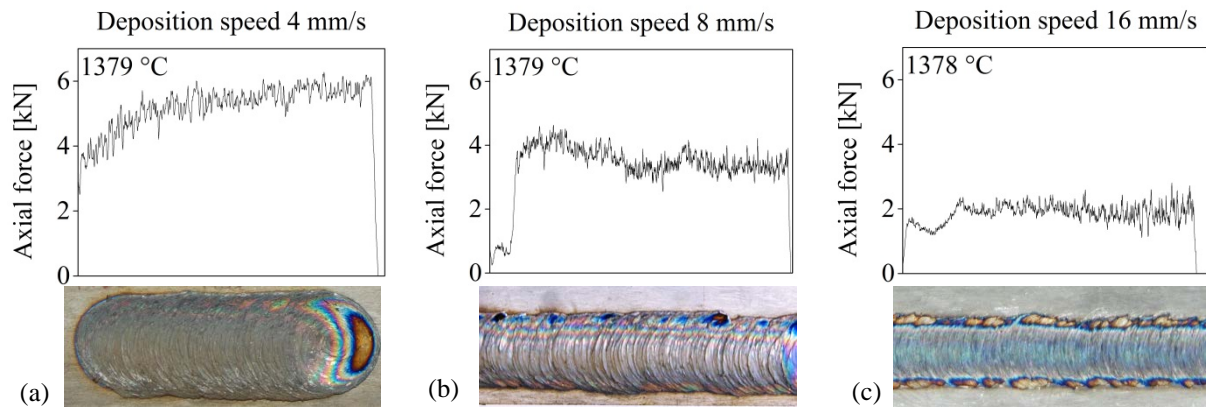


Figure 8: Axial force response to variation of the deposition speed when using 3000 min^{-1} rotational speed with corresponding temperature values and Ti-6Al-4V alloy coating images

The strain rate sensitivity is a crucial factor in plastic deformation of titanium alloys. Strain rate sensitivity can be defined as the ratio of incremental change in stress ($\log \sigma$) to the resultant change in strain rate ($\log \dot{\epsilon}$) at a given strain and temperature (Dieter (1961)). Furthermore, it has been reported that the strain rate sensitivity factor of titanium rises with increase in temperature and drops when increasing the strain rate (Rosen et al. (1999)). It is well known that titanium alloys tend to instable flow behaviour during plastic deformation. It seems that the temperature and deformation induced by the FS process in regime I influence the flow stress behaviour of the titanium coatings. This instable flow stresses result at times in unsteady material behaviour forming flash at the coating.

Park et al. (2002) have published the stress behaviour of Ti-6Al-4V alloy depending on variation of temperature (max. 1000 °C) and strain rate in hot forging experiments. The results indicate that the stress significantly increases with the strain rate at temperatures below β -transus. However, within the β field at a temperature of 1000 °C the stress values still increase with the strain rate but the differences become smaller (Figure 9) (Park et al. (2002)). Considering the increase in temperature with increasing rotational speed up to 1304 °C, which was measured in regime II, it might be assumed that the flow stress values might not vary significantly. Therefore, the material flow at the constant, high temperature in regime II can be assumed not to be strongly affected by changes in strain rate at the different rotational speeds. Possibly, dynamic recrystallization, which plays a major role at such high deformation, takes place in a steady state of equal rates dislocation generation and their reduction through recrystallization. The combination of high strain rates and fast dynamic recrystallisation in regime II might circumvent other thermal softening effects. At the low rotational speeds in regime I, both the temperature and strain rate vary at the same time, which may lead to considerable differences in the flow stresses. No literature is available on severe plastic deformation of Ti-6Al-4V alloy at the high strain rates and strains which take effect during Friction Surfacing, and further studies will be required for a comprehensive explanation of the flash formation behavior observed in the present study.

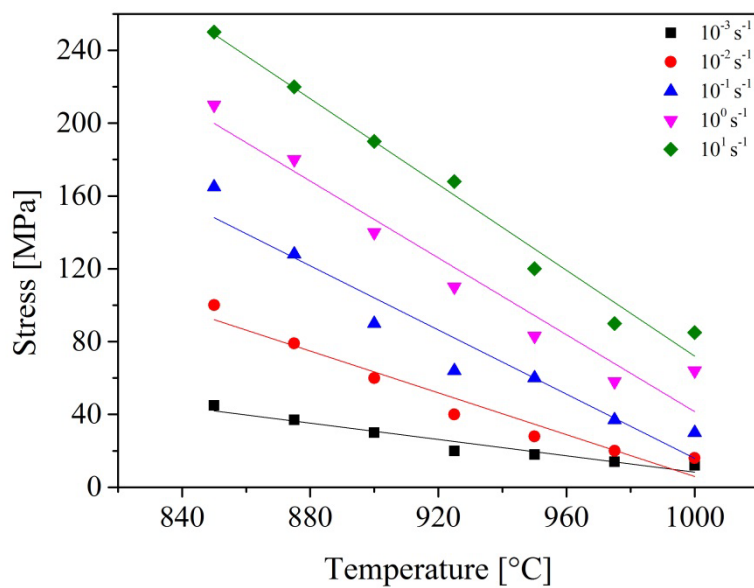


Figure 9: Influence of strain rates and temperatures on the flow stress of Ti-6Al-4V during hot forging according to Park et al. (2002)

1.4 Coating dimensions

The influence of deposition speed on the coating geometry in both rotational speed regimes was investigated. The coating thickness and width generated with various deposition speeds for two rotational speeds (400 min⁻¹ and 3000 min⁻¹) are demonstrated in Figure 10. Generally, it can be observed for both rotational speeds that a decrease in deposition speed leads to wider and thicker coatings. Similar results have been observed for different steels, demonstrating an increase in coating thickness and width when low deposition speed was employed (Macedo et al. 2010)). In regime I the low deposition speed led to high temperatures, resulting in a higher amount of deposited material (thick and wide coating). In regime II when a low deposition speed is employed, the rod material undergoes a higher number of rotations, which leads to a large amount of plasticized material, and consequently wider and thicker coatings. It can be concluded that the highest amount of material can be deposited using regime II, in which the temperature is constant.

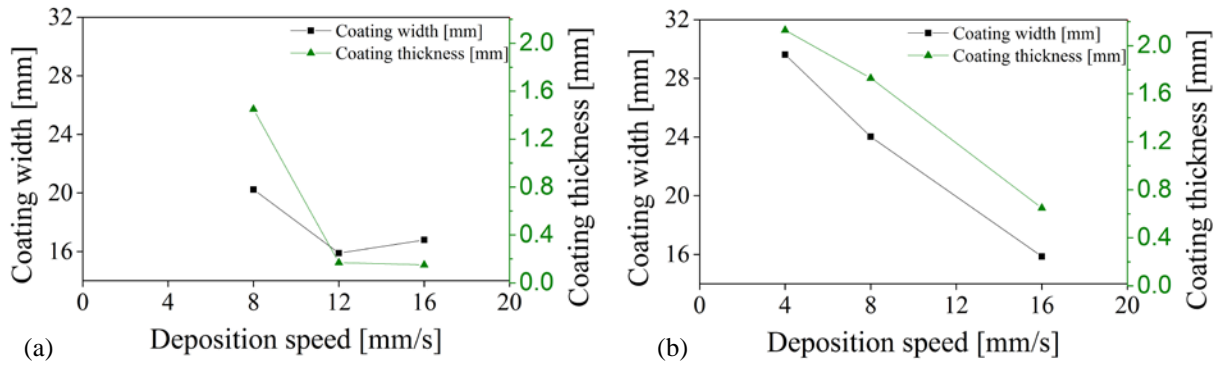


Figure 10: Effect of deposition speed on coating thickness and width using 400 min⁻¹ (a) and 3000 min⁻¹ (b) rotational speeds

1.5 Microstructure evolution

Ti-6Al-4V alloy undergoes a phase transformation to single β phase when reaching the transus temperature of 995 °C during heating. The microstructural features of Ti-6Al-4V alloy FS coatings differ after cooling, since martensitic phase transformation occurs under the high cooling rates. Since the rotational speed was varied in the current study, influencing the resultant temperature and cooling rates, an investigation of the microstructure formed at various processing condition was carried out.

The microstructure of the Ti-6Al-4V rod base material contains a dual-phase α - β structure, which exhibits equiaxed α grains with transformed β islands (Figure 11 a). The initial grain size of the rod base material is $4.42 \mu\text{m} \pm 2 \mu\text{m}$. The microstructure of a coating generated with 6000 min⁻¹ exhibiting a martensitic structure is shown in Figure 11 b. The prior β grain boundaries cannot be clearly distinguished.

The temperature measurements have revealed, that the Ti-6Al-4V alloy coatings have been deformed during the FS process in the β phase and were cooled through the α + β and the martensite phase regions (martensite start temperature is 800 °C). As it is well known, the phase transformation of Ti-6Al-4V while cooling can occur either martensitically or by the diffusion controlled nucleation and growth process. The phase transition depends on the cooling rate and the alloy composition. Generally, the martensitic transformation can be performed at cooling rates higher than 18 Ks⁻¹ and might lead either to the hexagonal crystal lattice (α') or orthorhombic crystal lattice (α'') (Lütjering and Williams (2007) and Sieniawski et al. (2013)). According to the temperature analysis and the determined cooling rates (39.8 Ks⁻¹ – 53.8 Ks⁻¹), which were higher than 18 Ks⁻¹, a diffusion controlled nucleation is precluded, and therefore it can be definitely stated that the phase transformation occurred martensitically.

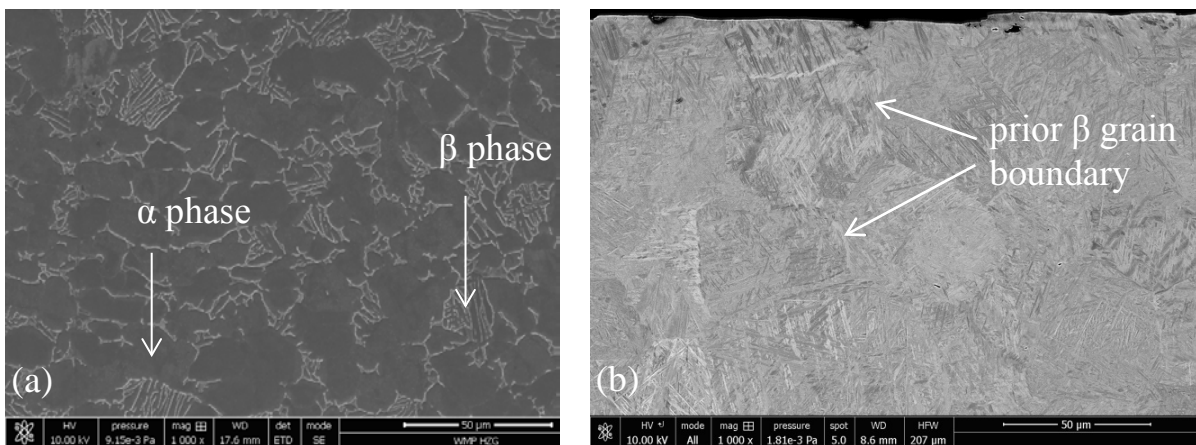


Figure 11: Microstructure of Ti-6Al-4V alloy rod in as-received condition (a) and of a coating produced with 6000 min⁻¹ (b)

In order to characterize the prior β grains formed at high temperature, grain size reconstruction was conducted as described in section 2. The reconstructed β grain size map for a coating generated with low rotational speed is shown in Figure 12. The prior β grain size of the coatings generated in regime I differs from the grain size in regime II (compare Figure 11 b and Figure 12 b).

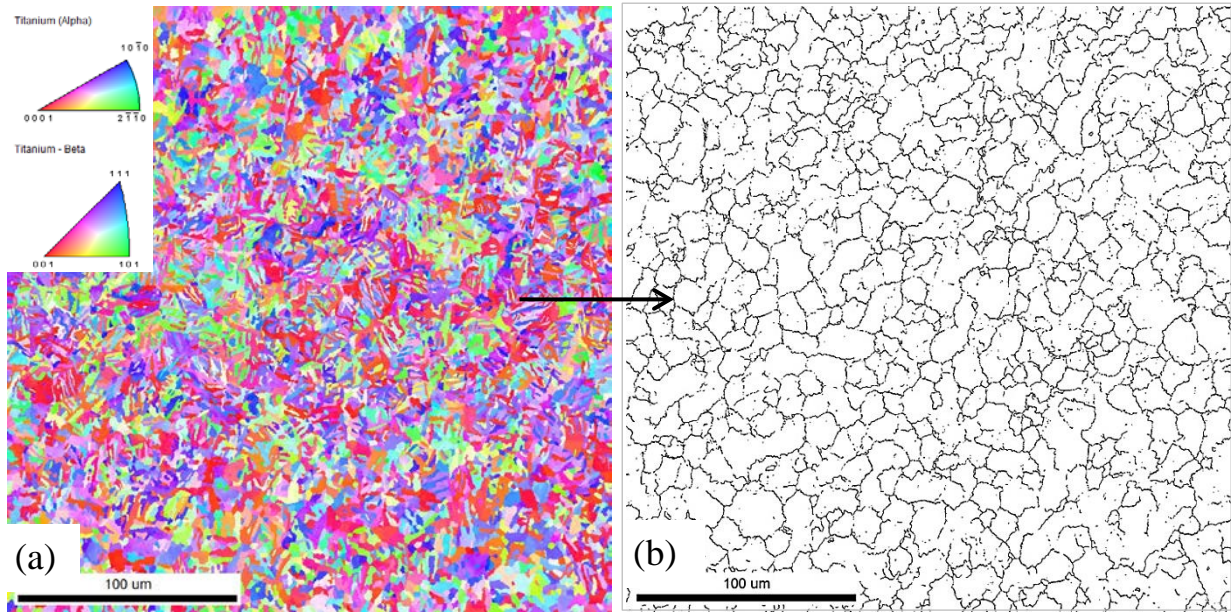


Figure 12: Inverse pole figure map of a coating generated with 400 min^{-1} rotational speed (a) and the corresponding reconstructed high temperature grain boundary black and white map (b)

The influence of the rotational speed on the grain size evolution is presented in Fig. 13. The coatings generated at low rotational speeds exhibit refined grains (Fig. 13 a, b) with 400 min^{-1} rotational speed measuring $1.64 \mu\text{m} \pm 1.33 \mu\text{m}$ (linear intercept length method). An increase in rotational speed (600 min^{-1}) and resultant temperature leads to a small increase in grain size. Coatings generated with 3000 min^{-1} and with a high peak temperature of $1298.3 \text{ }^\circ\text{C}$ demonstrate significantly coarser prior β grains of $28.43 \mu\text{m} \pm 11.47 \mu\text{m}$. From 3000 min^{-1} to 6000 min^{-1} no further grain size increase was observed; instead the grains size becomes slightly smaller (Fig. 13 c, d). Again, a clear threshold in regard to the two rotational speed regimes can be identified. In regime I grain refinement was observed, while in regime II coarse grains are formed. It can be concluded, that the combination of deformation rate and temperature affects the β grain size during Friction Surfacing.

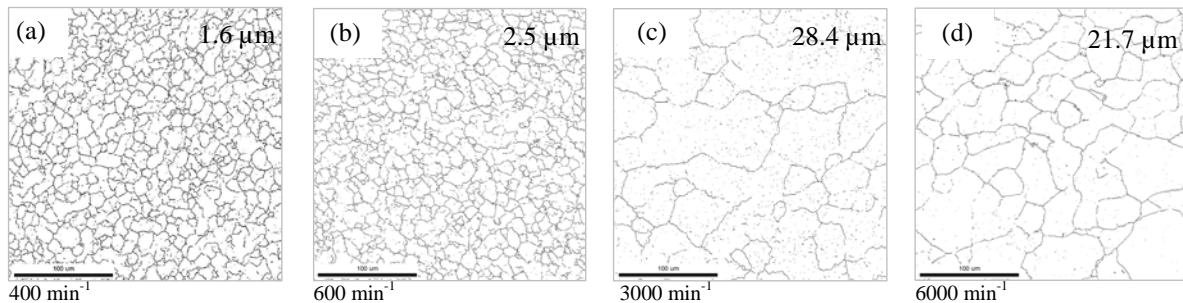


Fig. 13: Influence of the rotational speed on grain size evolution in Ti-6Al-4V alloy coatings. Reconstructed high temperature grain size is displayed on each black white map.

During Friction Stir Welding of Ti-6Al-4V the prior β grain size was found to increase, when varying the rotational speed from 300 min^{-1} to 600 min^{-1} in 100 min^{-1} steps. This grain size increase has been suggested to correlate with a higher heat input and corresponding temperature when raising the rotational speed. The increased temperatures (above the β Transus) lead to prolonged dwell time in the β phase which results in evolution of coarse grains (Zhang et al. (2008)). The same tendency of increasing β grain size for higher rotational speeds was found for FS, which can also be explained by the observed temperature rise.

1.6 Material deposition efficiency

As was shown in section 1.4, the rotational speed affects the coating geometry resulting in various coating widths and thicknesses. This finding leads to the inference that consequently the amount of the material loss (flash formation at the consumable rod) must also be affected by the variation in the rotational speed.

The material deposition efficiency is defined as the ratio of the deposited volume to the consumption volume of the rod and can be calculated as follows (Gandra et al. (2012)):

$$\eta_{\text{deposition}}(\%) = \frac{\text{Deposited volume}}{\text{Consumption volume of the rod}} * 100\%$$

The deposited volume is the product of the cross sectional area of the coating layer and the deposited coating length. The consumption volume of the rod is the product of rod cross sectional area and the consumed rod length. To accurately determine the deposition efficiency of the coatings with a flash, a cross section without flash was selected, because the flash cannot be considered effective deposition.

The results presented in Fig. 14, describe the effects of the rotational speed and resultant axial force on the deposition efficiency. The deposition efficiency is strongly affected by the change in rotational speeds, varying in a wide range between 9 % and 39 %. As expected, the layers that were generated with low rotational speeds (400 min^{-1} - 600 min^{-1}) exhibiting low coating thicknesses provided low deposition efficiencies in a range of 9 % - 12 %. High deposition efficiencies were achieved for coatings generated with high rotational speeds (2000 min^{-1} and 6000 min^{-1}) in a range from 26% to 39 %. It should be mentioned that the most efficient configuration has been achieved at a rotational speed of 3000 min^{-1} , for which the highest temperature was measured ($1379 \text{ }^{\circ}\text{C}$).

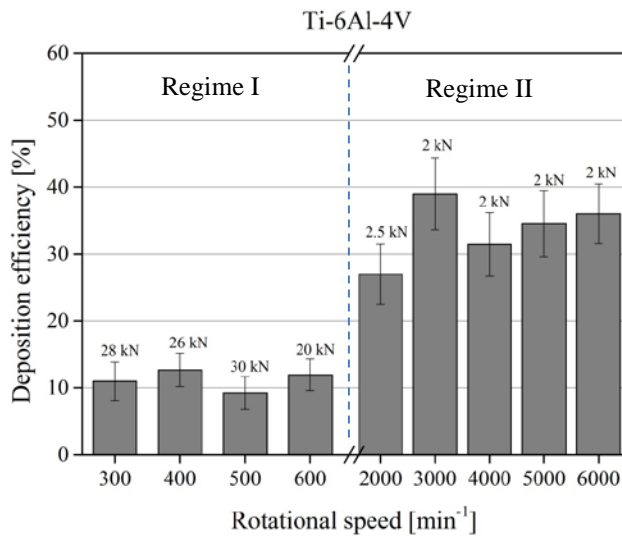


Fig. 14: Deposition efficiency of Ti-6Al-4V coatings as function of the rotational speed and resultant axial force exhibiting two clearly defined regimes.

The fact that low rotational speeds result in low efficiency and high rotational speeds result in high efficiency can again be related to the resultant axial forces. Under the low axial forces ($\sim 2 \text{ kN}$) at high rotational speeds less amount of the plasticized material was pushed into the flash in comparison to the coatings at low rotational speeds and high axial forces ($\sim 30 \text{ kN}$). Correspondingly, when a lower amount of material passes into the flash, a larger material amount can be deposited, increasing the deposition efficiency. Gandra et al. (2012) reported a similar relationship between the axial force and deposition efficiency in aluminium alloys, pointing out that a low axial force range results in effectively deposited material while the use of high forces provides low efficiency.

4. Conclusions

The results of this study have shown that rotational speed plays a major role in the process characteristics while depositing Ti-6Al-4V alloy coatings. Two different regimes with a threshold at 2000 min⁻¹ rotational speed were established in regards to material flow behaviour, coating geometry and grain size evolution.

- In regime I, flash generation at the coating may occur at certain combinations of the rotational and deposition speeds. Both parameters are responsible for the temperature development that affects the material flow stresses during deposition, resulting either in thermal softening (flash generated at the coating) or stable flow (flash formed at the rod).
- In regime II, the temperature achieves a steady-state condition. Here the flash generation at the coating is precluded and an alteration of rotational speed and deposition speeds do not significantly influence the temperature distribution.
- Temperature measurements have shown the peak temperature (in the range of 1021 °C - 1379 °C) exceeds β transus in all experiments. The temperature does not change while processing. The peak temperature and heating rate are affected by the rotational speed.
- Ti-6Al-4V alloy has been deformed in the β -phase. Here, during processing dynamic recrystallization took place. The phase transformation during cooling of the coatings occurs martensitically due to high cooling rate (46.4 Ks⁻¹). It has been shown that by using low rotational speed and thereby resultant low temperatures the high temperature β grains were refined compared to the base material. By raising the rotational speed the temperature increases and the grains become coarse. An additional rise in rotational speed without further increase of the temperature does not lead to additional grain growth.
- The fact that a selection of low rotational speeds results in low deposition efficiency and high rotational speeds result in high efficiency are related to the resultant acting axial forces. Under low axial forces (~2 kN) at high rotational speeds less amount of the material was pushed into the flash in comparison to the coatings at low rotational speeds and high axial forces (~30 kN). Therefore, the highest deposition efficiency of 39 % has been achieved with high rotational speeds (3000 min⁻¹ and 6000 min⁻¹).

Acknowledgements

Authors appreciatively acknowledge Henning Krohn for his assistance in operation of the Friction Surfacing machine and Carlos Alberto Belei Feliciano for his support in metallographic preparation.

References

- <http://www.frictec.com>. 2010.
- Dieter GE. Mechanical Metallurgy 1961.
- Fitseva V, Krohn H, Hanke S, dos Santos JF. Friction surfacing of Ti-6Al-4V: Process characteristics and deposition behaviour at various rotational speeds. *Surface and Coatings Technology*. 2015;278:56-63.
- Gandra J, Miranda RM, Vilaça P. Performance analysis of friction surfacing. *Journal of Materials Processing Technology*. 2012;212:1676-86.
- Gey N, Humbert M. Characterization of the variant selection occurring during the $\alpha \rightarrow \beta \rightarrow \alpha$ phase transformations of a cold rolled titanium sheet. *Acta Materialia*. 2002;50:277-87.
- Gey N, Humbert M. Specific analysis of EBSD data to study the texture inheritance due to the $\beta \rightarrow \alpha$ phase transformation. *Journal of Materials Science*. 2003;1289-94.
- Glavicic MG, Kobrun PA, Bieler TR, Semiatin SL. A method to determine the orientation of the high-temperature beta phase from measured EBSD data for the low-temperature alpha phase in Ti-6Al-4V. *Materials Science and Engineering A* 2003;A346:50-9.
- Hanke S, Beyer M, Silvonen A, dos Santos JF, Fischer A. Cavitation erosion of Cr60Ni40 coatings generated by friction surfacing. *Wear*. 2013;301:415-23.
- Hanke S, Fischer A, Beyer M, Dos Santos JF. Reibauftragschweißen von NiAl-Bronze-Verfahren und Materialeigenschaften unter Kavitation. *Metall-Forschung*. 2009.
- Khalid Rafi H, Janaki Ram GD, Phanikumar G, Prasad Rao K. Microstructure and Properties of Friction Surfaced Stainless Steel and Tool Steel Coatings. *Materials Science Forum*. 2010;638-642:864-9.
- Lütjering G, Williams JC. *Titanium* 2007.
- Macedo MLK, Pinheiro GA, dos Santos JF, Strohaecker TR. Deposit by friction surfacing and its applications. *Welding International*. 2010;24 No.6.
- Mironov S, Zhang Y, Sato YS, Kokawa H. Development of grain structure in β -phase field during friction stir welding of Ti-6Al-4V alloy. *Scripta Materialia*. 2008;59:27-30.
- Park NK, Yeom JT, Na YS. Characterization of deformation stability in hot forging of conventional Ti-6Al-4V using processing maps. *Materials and Processing Technology*. 2002.
- Puli R, Janaki Ram GD. Corrosion performance of AISI 316L friction surfaced coatings. *Corrosion Science*. 2012;62:95-103.

- Rafi HK, Ram GDJ, Phanikumar G, Rao KP. Friction Surfacing of Austenitic Stainless Steel on Low Carbon Steel: Studies on the Effects of Traverse Speed. 2010;2.
- Rao KP, Damodaram R, Rafi HK, Ram GDJ, Reddy GM, Nagalakshmi R. Friction surfaced Stellite6 coatings. *Materials Characterization*. 2012;70:111-6.
- Rosen RS, Paddon SP, Kassner ME. The Variation of the Yield Stress of Ti Alloys with Strain Rate at High Temperatures. *Journal of Materials Engineering and Performance*. 1999.
- Sieniawski J, Ziaja W, Kubiak K, Motyk M. Microstructure and Mechanical Properties of High Strength Two-Phase Titanium Alloys. 2013.
- Suhuddin U, Mironov S, Krohn H, Beyer M, dos Santos JF. Microstructural Evolution During Friction Surfacing of Dissimilar Aluminum Alloys. *Metallurgical and Materials Transactions A*. 2012;43:5224-31.
- Zhang Y, Sato YS, Kokawa H, Park SHC, Hirano S. Microstructural characteristics and mechanical properties of Ti-6Al-4V friction stir welds. *Materials Science and Engineering: A*. 2008;485:448-55.